TRANSPORT OF DECAY PRODUCTS IN THE BETA-BEAM DECAY RING*

A. Chancé †, J. Payet, CEA, IRFU, SACM, F-91191 Gif-sur-Yvette, France.

Abstract

The principle of the neutrino production in the beta-beams relies on the beta-decay of the radioactive ions Neon 18 and Helium 6 in a storage ring. After decaying, the daughter particles have their magnetic rigidity significantly changed (-33 % for Helium and +11 % for Neon). Therefore, the decay products will be quickly lost on the walls of the decay ring after entering a dipole. Absorbers have been inserted in the decay ring in order to collect most decay products. Their optimization implies to calculate the trajectories of the decay products in the dipoles for very large momentum differences with a good accuracy. For pure dipoles without fringe field as in the decay ring, an analytic treatment can be used to simulate the transport. It is then possible to obtain the equivalent dipole which gives the beam sizes of the daughter particles. In a first part, we will describe the analytic treatment of the central trajectory and the motion of the ions around. In a second part, we will compare this treatment with the one with matrices for different orders in the case of the beta-beam decay ring.

INTRODUCTION

The Beta-Beam decay ring is the final stage of the accelerator complex comprising the baseline design [1, 2] of the EURISOL Beta Beam Task [3]. After being produced in an ISOL front end, β radioactive ions $^6\mathrm{He}^{2+}$ and $^{18}\mathrm{Ne}^{10+}$ are accelerated up to $\gamma = 100$ to be injected in the decay ring. The radioactive ions are then stored until decaying or being lost in another process. One of the main problematics of the decay ring is to manage the high intensities of the daughter particles $^6\mathrm{Li}^{3+}$ and $^{18}\mathrm{F}^{9+}$ due to the β decay of the reference beam [4, 5]. Indeed, the magnetic rigidity of the decay products is significantly different from the one of the reference beam as the Table 1 shows it. These ions will be quickly lost and will impinge the walls, which can limit the maintenance or provoke quenches in the superconducting magnetic elements. A proposed solution was to insert absorbers in the structure. The optimization of the magnetic elements to handle the decay losses was presented in [4].

* Work supported by European Community under the FP6 - Research Infrastructure Action - Structuring the European Research Area - EURISOL DS Project Contract no. 515768 RIDS.

† achance@cea.fr

Table 1: Magnetic rigidity of the decay products in the β beam Decay Ring

Mother particle			Decay product		
Ion	Charge	γ	Name	Charge	$\frac{\Delta(B\rho)}{B\rho}$
^{6}He	$+2$	100	^{6}Li	$+3$	-0.3338
^{18}Ne	$+10$	100	^{18}F	$+9$	$+0.1109$

TRAJECTORY OF THE IONS IN THE DIPOLES

Case of a Pure Sector Magnet

In the case of pure dipole sector magnets, we know that the trajectory of the particles are circle arcs. The idea is to calculate precisely the trajectory of the ions by using geometrical considerations, which gives then the parameters of the equivalent dipole. A layout of the trajectory in the dipole is represented on Fig. 1. In the following, we will use the notations below :

ρ, θ	the reference bending radius and angle of the dipole.
$L = \rho\theta$	the dipole length.
$\delta = \frac{\Delta(B\rho)}{B\rho}$	the relative magnetic rigidity difference.
ρ^*, θ^*	the bending radius and angle of the equivalent dipole.
(x_0,xp_0,y_0, yp_0,l_0,δ)	the $6D$ coordinates of the ion at the dipole entry.
α_0	the horizontal angle of the ion at the dipole entry.
(x_1,xp_1,y_1, yp_1,l_1,δ)	the $6D$ coordinates of the ion at the dipole exit.
α_1	the horizontal angle of the ion at the dipole exit.
L^*	the path length.

After calculation, we have :

$$\begin{aligned}
\rho^* &= \rho(1+\delta)\sqrt{\tfrac{1+xp_0^2}{1+xp_0^2+yp_0^2}} \\
\alpha_1 &= \arcsin\left(\tfrac{\rho+x_0}{\rho^*}\sin\theta - \sin(\theta-\alpha_0)\right) \\
\theta^* &= \theta - \alpha_0 + \alpha_1 \\
x_1 &= \rho^*\tfrac{\sin(\theta^*+\alpha_0)-\sin\alpha_0}{\sin\theta} - \rho \\
xp_1 &= -\tan\alpha_1 \\
L^* &= \rho^*\theta^*
\end{aligned}$$

The advantage is to have an exact formulation of the transport in a pure dipole magnet. It is then possible to find the transport matrix around the ion trajectory by doing a Taylor-Lagrange development of the formulæ above. That gives the evolution of the beam sizes of the decay product inside the dipole too.

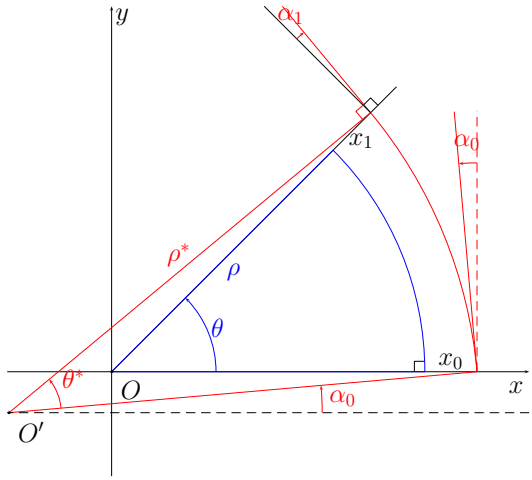

Figure 1: Layout of the transport of an ion in a pure dipole field. In blue, reference particle.

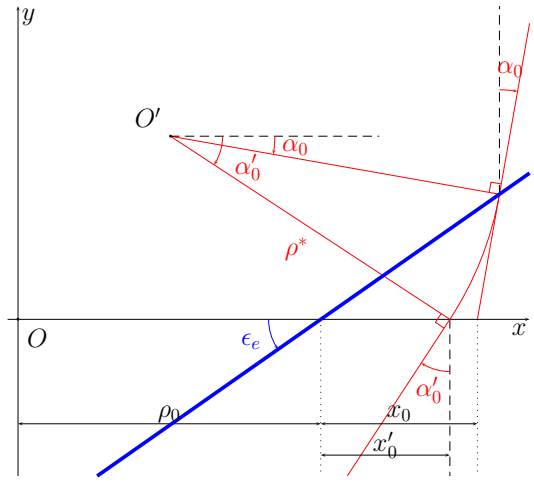

Figure 2: Layout of the transport of an ion in an entry edge (in blue). The axis (Ox) corresponds to the entry face with $\epsilon_e = 0$.

Treatment of the Entry and Exit Edges

In the preceding subsection, we have considered the dipole as a sector magnet with its faces perpendicular to the reference orbit. In the case of non perpendicular faces, we have to take into account an error on the magnetic field integrand. Geometrically, it is translated by calculating the coordinates that the ion should have to keep the same trajectory in the case of perpendicular faces.

We will note ϵ_e and ϵ_s the respective angles of the entry and exit faces, α'_0 and x'_0 the new coordinates of the ion to use after the entry edge, α'_1 and x'_1 the new coordinates of the ion to use after the exit edge. The geometry at the entry and exit edges is respectively represented on the Figs. 2 and 3. Finally, we find the following relations :

$$\begin{aligned}
\alpha'_0 &= \arcsin\left(\sin\alpha_0 - \tfrac{\tan\epsilon_e}{1+\tan\alpha_0\tan\epsilon_e}\cdot\tfrac{x_0}{\rho^*}\right)\\
x'_0 &= \tfrac{1}{1+\tan\alpha_0\tan\epsilon_e}x_0 + \rho^*\cdot(\cos\alpha'_0 - \cos\alpha_0)\\
\alpha'_1 &= \epsilon_S + \arcsin\left(\sin(\alpha_1-\epsilon_s) + \tfrac{x_1}{\rho^*}\cdot\sin\epsilon_s\right)\\
x'_1 &= x_1 + \tfrac{\rho^*}{\cos\alpha'_1}\left(1-\cos(\alpha'_1-\alpha_1)\right)
\end{aligned}$$

A Taylor-Lagrange development of the formulæ above enables to find the transport matrix again. These relations are only available if the fringe field effects are neglected.

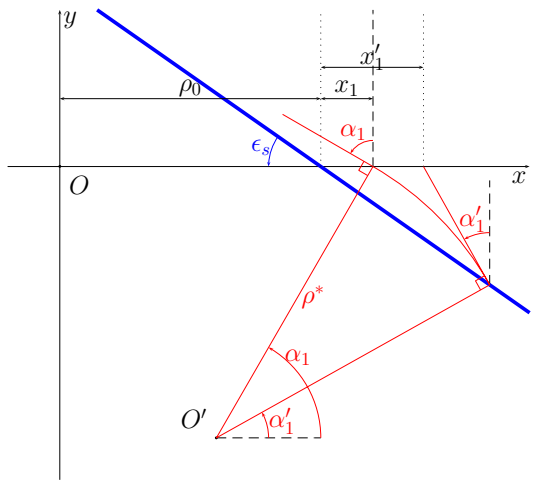

Figure 3: Layout of the transport of an ion in an exit edge (in blue). The axis (Ox) corresponds to the exit face with $\epsilon_s = 0$.

COMPARISON WITH DIFFERENT TRANSPORT CODES

In order to verify the availability of the model, decay products have been transported with different codes: first, second and third order transport with TRANSPORT code [7], transport with BETA [6] with the new treatment of the dipole and transport with MADX [8] by using the integration of PTC [9]. We have assumed that the decay occurred at the entry of the dipoles. The trajectory of the decay products from Helium are drawn on Fig. 4 and from Neon on Fig. 5. The dipole angle is equal to $\theta = \pi/86$ rad and its curvature radius is $\rho = 156$ m. It appears that in both cases, the first order is not sufficient to describe properly the trajectory of the decay products. However, whereas the second order is sufficient in the Fluorine case, it is not true for Lithium. The development must be done up to third order and further. Moreover, we have an excellent agreement between PTC and the new treatment of the dipoles in BETA.

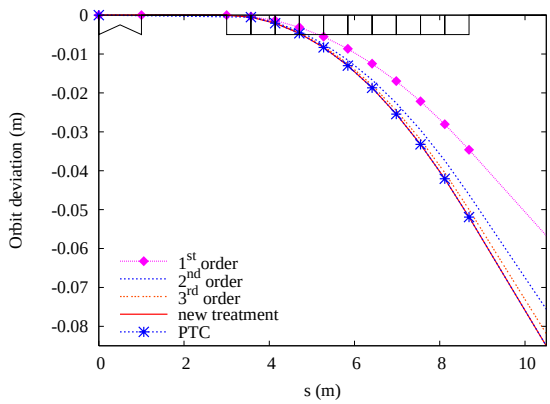

Figure 4: Comparison of the trajectories of the decay products from $^{6}He^{2+}$ in a dipole in the case of a first, second and third order transport with TRANSPORT, of a transport with PTC and with the new treatment of the dipoles with BETA.

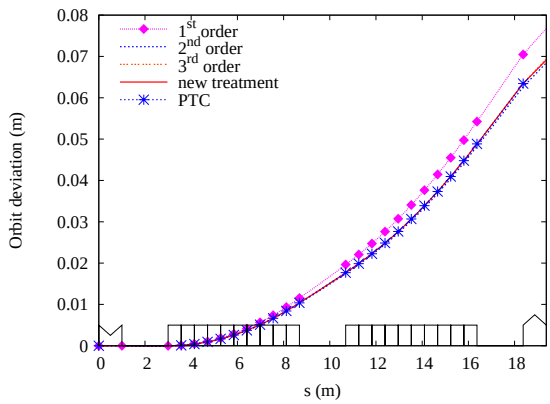

Figure 5: Comparison of the trajectories of the decay products from $^{18}Ne^{10+}$ in a dipole in the case of a first, second and third order transport with TRANSPORT, of a transport with PTC and with the new treatment of the dipoles with BETA.

DEPOSITION OF THE DECAY PRODUCTS

In [4], we have presented the algorithm in BETA which evaluates in first approximation the deposition of the decay products on the absorbers. It consists in a transport of beam sizes along the structure and in an evaluation of the deposition which occurs in each element. The beam distribution is assumed to be Gaussian with an horizontal emittance of 0.22 mm.mrad. We have used the same lattice and the same chamber size but by using the analytic formulæ instead of a second order development. The transport in the quadrupoles was made by scaling their strength, which means dividing their focusing strength by the factor $(1 + \delta)$.

Only, the Helium case was considered because the difference between the two treatments is negligible in the Neon case. The results are given on the Fig. 6. The difference between the two models is very slim. The deposition occurs a bit earlier in the dipoles with the new treatment because the deviation of Lithium was underestimated at second order.

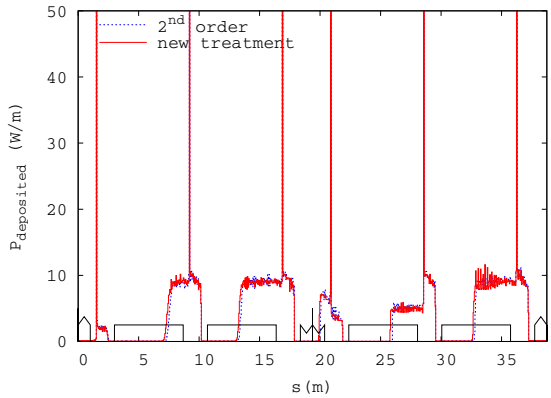

Figure 6: Deposition of the decay products Lithium on the wall. The chamber size is ± 80 mm for the magnetic elements and the absorbers are at 35 mm from the machine axis.

CONCLUSION

We have presented a new treatment of the transport in BETA for sector magnets according to the hard edge model. The fringe field is not taken into account and the dipoles are assumed without any index. Then, we have applied this model to the transport of the decay products in a dipole of the beta-beam decay ring. The comparison with other codes have shown a great agreement of the model and that it is necessary to consider the transport up to third order. Finally, we have used this model to consider the decay losses in a FODO lattice of the decay ring.

REFERENCES

[1] M. Benedikt, S. Hancock and M. Lindroos, Baseline Design for a Beta-Beam Neutrino Facility, EPAC'04, Lucerne, June 2004.

[2] Parameter and Intensity Values, Version 2, July 2005 (docversion), EURISOL DS/TASK12/TN-05-03.

[3] `http://beta-beam.web.cern.ch/`

[4] A. Chancé and J. Payet, Loss Management in the Beta-Beam Decay Ring, EPAC'06, Edinburgh, June 2006.

[5] F.W. Jones and E. Wildner, Simulation of Decays and Secondary Ion Losses in a Betabeam Decay Ring, PAC'07, Albuquerque, June 2007.

[6] BETA code, J. Payet

[7] K.L. Brown et al., Transport, a Computer Program for Designing Charged Particle Beam Transport Systems. See yellow reports CERN 73-16 (1973) & CERN 80-04 (1980).

[8] MAD-X, `http://mad.web.cern.ch/mad/`

[9] E. Forest et al., KEK Report No. 2002-3.